

Data Assimilation Experiments of Nerima Heavy Rainfall

Hiromu Seko^{*a}, Takuya Kawabata^a, Tadashi Tsuyuki^b

^a Meteorological Research Institute, Japan Meteorological Agency, Tsukuba, Japan

^b Numerical Prediction Division, Japan Meteorological Agency, Tokyo, Japan

1. Introduction

Because the thunderstorms in the urban areas sometimes cause the heavy rainfall, the precise forecast of their generation and development is needed. It is well known that the low-level convergence of moist air generates and develops the thunderstorms. Thus, it is expected that assimilation of the low-level convergence and moist air improves the forecast of the thunderstorms. In this study, the radial wind (RW) observed by Doppler radar and precipitable water vapor (PWV) derived from ground-based GPS were used as the assimilation data. When these data were assimilated by 4-dimensional data assimilation system for Mesoscale Spectral Model (MSM-4dVarDAS) of Japan Meteorological Agency (JMA), the time, position and shape of the precipitation regions that included the heavy rainfall at Nerima/Tokyo was reproduced. However, the precipitation intensity was much weaker than the observed one.

To reproduce intensity of the heavy rainfall, the non-hydrostatic model of JMA (NHM) that predicts water substances explicitly was used, and the RW and PWV was assimilated into NHM by 3-dimensional data assimilation system (NHM-3dVarDAS).

2. 'Nerima heavy rainfall'

On 21 July 1999, the Baiu front over the northern part of the Japan moved southward slowly. When the precipitation of the Baiu front entered the Kanto region, the convective system that had a horizontal scale of several ten kilometers was generated at the southern Kanto area at 15JST (Fig. 1). This convective system developed and the heavy rainfall of 111.5 mm/hour was observed at Nerima/Tokyo at about 16JST. When the intense convections were developed, the easterly and northerly flows were observed in the precipitation regions. The southwesterly inflow from the south converged with them along the southern edge of the precipitation regions. These precipitation regions began to decay from 17JST and weak precipitation areas remained until 21JST.

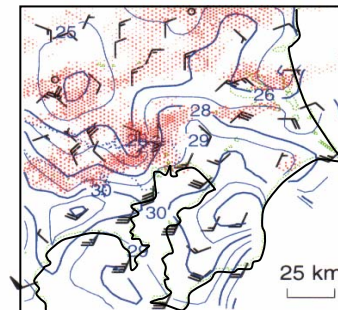


Fig. 1 Horizontal distribution of precipitation region (shade), surface temperature (solid line) and horizontal wind at 16JST 21 July

3. Impacts of RW and GPS-derived PWV

Because the heavy rainfall over the southern Kanto area was composed of well-developed convective cells, the horizontal grid interval of NHM was set to be 5km express the individual convective cells. Horizontal grid number was set to be 122 × 122 so that the simulation domain covered the whole Kanto area. Number of vertical layers was 45. The depth of the layer was stretched from 20 m to 1450 m from the surface to the upper boundary.

When the simulation was performed by NHM from the initial fields produced from the MSM-4dVarDAS-derived analyzed fields, however, the intense precipitation was not generated over the southern Kanto (not shown). Although the convergence of the horizontal wind was reproduced by MSM-4dVarDAS, the updraft estimated from spatial interpolated horizontal wind was too weak to saturate the water vapor. So as to reproduce intense updraft, RW observed by Doppler radars was assimilated into the initial fields of 15 JST by NHM-3dVar-DA system (Miyoshi, 2003). The production methods for assimilation data and observation operator are almost same as Seko et al., 2002, although observation errors of RW and PWV were reassessed.

The precipitation fields predicted from the results of NHM-3dVarDAS are shown in Fig. 2. The analyzed field at 15 JST shows that the southerly wind converged at the southern Kanto area. However, precipitation was not generated though the updraft was strengthened.

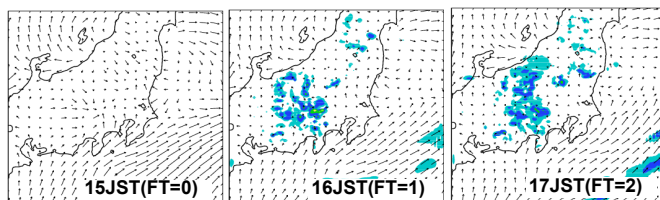


Fig. 2 Hourly precipitation and horizontal wind at 0.5 km from 15 JST to 17 JST on 21 July 1999 predicted by NHM.

4. Introduction of convective-cell-scale water vapor distribution and initial rain water and snow

In NHM-3DVarDAS, water vapor was not related to the updraft velocity to avoid the generation of unrealistic waves over the mountain areas. Therefore, water vapor in the intense updraft regions was not always saturated by NHM-

* hseko@mri-jma.go.jp, phone +81-29-853-8640; fax +81-29-853-8649

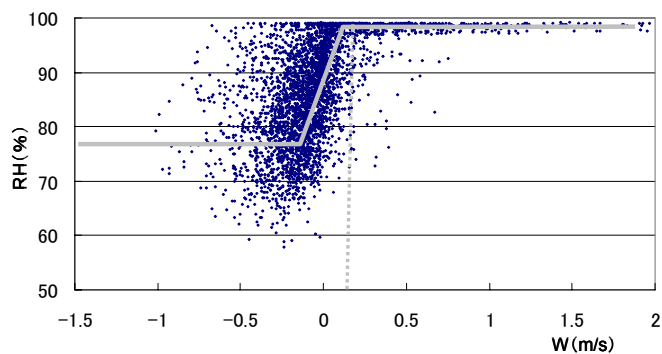


Fig.3 Scatter gram of simulated RH and updraft velocity within the precipitation region in the ranges of Doppler radar produced from the output of the NHM.

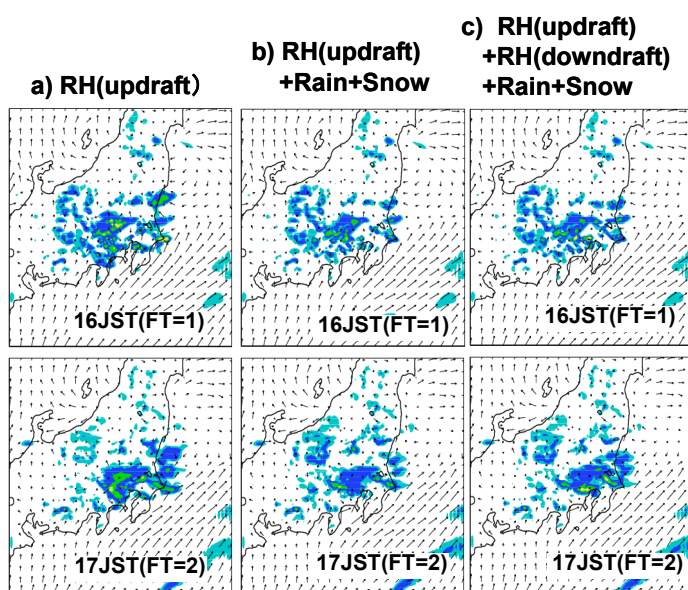


Fig. 4 Impact of introducing the convective cell scale water vapor distribution and initial water substances.

vapor and initial water substances. When the rain water and snow were introduced, the northwestern part of the precipitation region, which was decaying at 17 JST, was well reproduced. Furthermore, when the RH at the downdraft grids was changed, the convections along the southern edge of the precipitation region, which were produced by the outflow from the decaying region, were more developed. These simulated features were common to the observed ones. These similarities of precipitation intensity were maintained until 20 JST.

5. Summary

In these data assimilation experiments, the impacts of convective-cell-scale water vapor and the initial water substances on the precipitation prediction of a heavy rainfall were investigated. The comparison with the observed precipitation field indicates that convective-cell-scale water vapor and the introducing the rain water and snow should be considered in reproducing the convective cells of heavy rainfall.

References

- Miyoshi, T. "Development of JNoVA0 (three dimensional data assimilations system)", *Suuchiyohouka-houkoku, bettusatsu* **49**, pp148-155, 2003 (in Japanese)
- Ishikawa, Y., "Development of a mesoscale 4-dimensional variational data assimilation (4D-Var) system at JMA". *Proc. of the 81st Annual Meeting of AMS: Precipitation Extremes: Prediction, Impacts, and Responses*, P2.45, 2001.

3DVarDAS. In order that the relation between water vapor and updraft velocity is given to the analyzed fields, the scatter gram of simulated Relative humidity (RH) and updraft velocity within the precipitation regions within the radar ranges was obtained from the outputs of the NHM (Fig. 3). Because water vapor where the updraft exceeded 1.5 m/s was saturated, water vapor at updraft grids within the observed precipitation region was set to be saturated. This relation also means that intense updraft was maintained by convections. When the numerical simulations were performed from this modified initial condition, precipitation over the southern Kanto area was reproduced (Fig. 4a). However, the northwestern part of the precipitation region developed too intensely, while the observed northwestern part was decaying at 15 JST. This overdeveloped precipitation was due to the relation between the RH and updraft velocity that cannot express the evolution of convections.

So as to express the evolution of convective cells, rain water, snow and RH in the downdraft region were introduced. In general, there is large amount of rain water and snow, which weaken the updraft, in the well-developed convections. Thus, rain water and snow were estimated from the observed reflectivity fields, and then portioned according to the analyzed temperature. Namely, if the temperature was below 0 degree, snow was given at the grid points where the reflectivity was observed. It is known that the low-level cold outflow was produced by evaporation of water substances in dry downdraft regions. The low-level cold outflow helps develop the intense convections through the intensification of low-level convergence. Thus, the relation between the RH and downdraft was also obtained from the scatter gram, and then the RH in the downdraft region within the precipitation regions was changed according to the relation. Figures 4b and 4c show the impacts of introducing the convective-cell-scale water